# PCCP

Physical Chemistry Chemical Physics

rsc.li/pccp
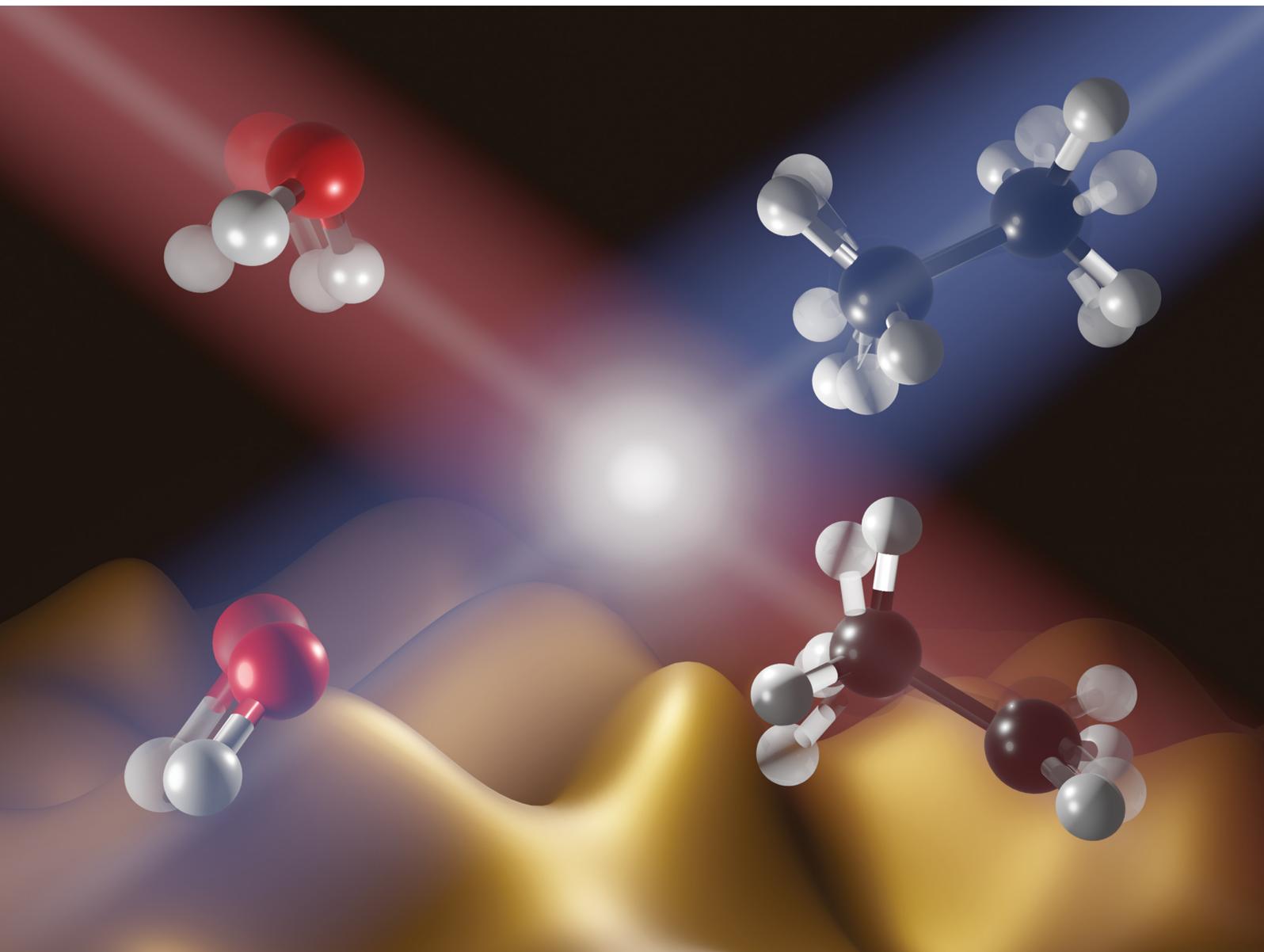
ROYAL SOCIETY
OF CHEMISTRY

**PERSPECTIVE**
Gábor Czakó *et al.*
First-principles mode-specific reaction dynamics

PCCP
Owner Societies

# PCCP

## PERSPECTIVE

Check for updates

# First-principles mode-specific reaction dynamics

Gábor Czakó, [ID] * Balázs Gruber, Dóra Papp, [ID] Viktor Tajti, [ID] Domonkos A. Tasi [ID] and Cangtao Yin [ID]

Controlling the outcome of chemical reactions by exciting specific vibrational and/or rotational modes of the reactants is one of the major goals of modern reaction dynamics studies. In the present Perspective, we focus on first-principles vibrational and rotational mode-specific dynamics computations on reactions of neutral and anionic systems beyond six atoms such as $X + C_2H_6$ [X = F, Cl, OH], $HX + C_2H_5$ [X = Br, I], $OH^- + CH_3I$, and $F^- + CH_3CH_2Cl$. The dynamics simulations utilize high-level *ab initio* analytical potential energy surfaces and the quasi-classical trajectory method. Besides initial state specificity and the validity of the Polanyi rules, mode-specific vibrational-state assignment for polyatomic product species using normal-mode analysis and Gaussian binning is also discussed and compared with experiment.

## I. Introduction

Energy efficiency is a fundamental question at many fields of basic and applied sciences. Physical chemists aim to understand this question at the deepest atomic and molecular level. One can invest energy into chemical reactions *via* translational,

*MTA-SZTE Lendület Computational Reaction Dynamics Research Group, Interdisciplinary Excellence Centre and Department of Physical Chemistry and Materials Science, Institute of Chemistry, University of Szeged, Rerrich Béla tér 1, Szeged H-6720, Hungary. E-mail: gczako@chem.u-szeged.hu*

vibrational, and rotational excitations of the reactants and the reactive system can utilize the different forms of energy with different efficiency. The so-called Polanyi rules[1] say that translational energy activates early-barrier, reactant-like transition-state-controlled reactions more efficiently than vibrational excitation, whereas the reverse is true in the case of late-barrier processes, which have product-like transition states. However, Polanyi uncovered these rules for simple reactions of atoms with diatomic molecules, where the reactants have only one vibrational degree of freedom.[1] Polyatomic molecules have different vibrational modes corresponding to various stretching



*Gábor Czakó received his PhD at Eötvös University (2007) and became a postdoc at Emory University (2008–2011), then a research associate at Eötvös University (2011–2015). He is currently an associate professor and the head of the MTA-SZTE Lendület Computational Reaction Dynamics Research Group at the University of Szeged. His current research involves PES developments, reaction dynamics, and ab initio thermochemistry. He received*

**Gábor Czakó**

*the Polanyi Prize (2012), Junior Prima Prize (2012), DSc (2017), habilitation (2018), Science Prize of the Faculty (2018), and University Prizes Young Researcher (2020) and Publication of the Year (2022) and published in Science, PNAS, Nature Chemistry, and Nature Communications.*



**Balázs Gruber**

*Balázs Gruber received his BSc and MSc degrees in chemistry at the University of Szeged in 2018 and 2020, respectively. In 2020 he won the Research Student Competition of the Institute of Chemistry. Currently, he is a fourth-year PhD student in the field of theoretical chemistry supervised by Gábor Czakó, and a second-year BSc student in computer sciences at the University of Szeged. His current research focuses on investigating the reactions of the hydroxyl radical, such as ethane + OH, methylamine + OH, and glycine + OH.*

**15818** | *Phys. Chem. Chem. Phys.*, 2024, **26**, 15818–15830

This journal is © the Owner Societies 2024

and bending motions, which may have specific effects on the reactivity. Vibrational mode specificity was first revealed in 1984 by quasi-classical trajectory (QCT) computations for the H + HOD reaction.[2] The simulations showed that excitation of the OH stretching mode of the reactant significantly enhances the $H_2$ + OD channel.[2] This theoretical finding was later confirmed by the experiments of the Crim[3,4] and Zare[5] groups in the early 1990s, which was a nice demonstration of the predictive power of theoretical reaction dynamics studies. The first fully quantum simulation of a polyatomic chemical reaction was performed by Zhang and Light in 1997 underpinning the mode specificity of the H + HOD reaction.[6]

The next important step in the mode-specific chemistry was the investigation of the reactions of H, F, and Cl atoms with methane ($CH_4$, $CHD_3$, etc.).[7–20] From the theoretical part, Espinosa-García and co-workers[8] pioneered with their semi-empirical potential energy surface (PES)-based QCT simulations and Bowman and co-workers with their reduced-dimensional quantum computations,[9] as well as with QCT studies on fully *ab initio* permutationally-invariant PESs.[12] From the experimental side we should mention again Crim[11] and Zare[7] and their co-workers. Furthermore, in 2003 the Liu group[21] set a new state-of-the-art for crossed-beam velocity-map-imaging of chemical reactions by measuring correlated product vibrational distributions for the $F + CD_4 \rightarrow DF + CD_3$ reaction. This experimental technique was later used for the Cl + $CHD_3$ and F + $CHD_3$ reactions revealing departures from the Polanyi rules[14] and unexpected CH stretching effects hindering CH bond cleavage,[16] respectively. Following a few

*Dóra Papp received her PhD in theoretical chemistry at Eötvös University, Budapest in 2018, then joined Prof. Gábor Czakó's group as a postdoc at the University of Szeged. Before graduating she did research in computational biochemistry, won the Hungarian-Republic Scholarship and University Competition of Research Students, and completed a 6-months research project at Chalmers University, Gothenburg. During her PhD work she*

**Dóra Papp**

*developed and applied a code analyzing molecular rovibrational resonances. Her postdoctoral research involves PES development and dynamics studies of atom + ethane and N/P-centered $S_N2$ reactions. In 2022 she started a postdoc with Prof. Hua Guo on metal surface dynamics.*

*Viktor Tajti received his BSc in molecular bionics engineering and MSc in info-bionics engineering at the University of Szeged, Hungary, in 2017 and 2019, respectively. In 2018 he took 2nd place at the University Competition of Research Students. In 2023 he successfully defended his PhD dissertation. The main subject of his research is the dynamics of the $F^- + CH_3CH_2Cl$ reaction. He is currently a postdoc at the University of*

**Viktor Tajti**

*Szeged in the group of Gábor Czakó. He has implemented several computer codes used in the group and continues his research on developing theoretical methods to investigate reaction dynamics.*

*Domonkos A. Tasi obtained his BSc and MSc degrees in chemistry at the University of Szeged, Hungary, in 2015 and 2017, respectively. During his undergraduate studies he worked on an alternative interpretation of toxicity of metal oxide nanoparticles towards bacteria E. coli. Then he joined the Computational Reaction Dynamics Research Group and received his PhD in 2023. His current research interests involve benchmark ab*

**Domonkos A. Tasi**

*initio and dynamics studies on $S_N2$ reactions focusing on novel retention pathways and oxide-ion substitution. He has received the National Young Talent Scholarship three times, and has obtained the Talent Scholarship in the PhD category.*

*Cangtao Yin obtained his PhD degree at Tianjin University, focusing on reaction rate theories including transition state theory, collision theory etc., in the framework of statistical mechanics. Then he joined the Institute of Atomic and Molecular Sciences, Academia Sinica as a postdoc under the guidance of Kaito Takahashi, studying quantum chemistry, with an emphasis on the Criegee intermediate-related reactions in the atmospheric*

**Cangtao Yin**

*conditions. He joined Gábor Czakó's group as a postdoctoral researcher at the University of Szeged, Hungary in 2022. His current research interest involves potential energy surface development and quasi-classical dynamical simulations.*

This journal is © the Owner Societies 2024

*Phys. Chem. Chem. Phys.*, 2024, **26**, 15818–15830 | **15819**

earlier theoretical studies on atom + methane systems,[8–10,12,13,15] the first author of the present article started to investigate the mode-specific dynamics of the $F/Cl/O + CHD_3$ reactions as a postdoc in the Bowman group about 15 years ago.[17–20] We developed analytical PESs by fitting high-level *ab initio* energy points, allowing efficient QCT simulations.[20] Our PESs and simulations[18,22] provided new insights into the Liu experiments[14,16] and led to several collaborative theoretical-experimental studies with Liu and co-workers[23–26] as well as QCT-quantum studies with the groups of Zhang,[19] Guo,[26,27] and Yang.[26,27]

By the 2010s vibrational mode specificity had been thoroughly studied, however, much less was known about the effect of the initial rotation on the reactivity, especially in the case of a polyatomic reactant. The rotational motion of a polyatomic molecule can be characterized by the quantum number $J$ corresponding to the total rotational angular momentum and its projection(s) to various principal axes resulting in $K_a$ and $K_c$ quantum numbers for asymmetric and $K$ for symmetric tops. Different $K$ values correspond to different types of rotation, for example, $K = 0$ and $K = J$ mean tumbling and spinning motion, respectively. Following our previous collaborative experimental-theoretical work on $Cl + CHD_3(JK)$, we call these rotational states as rotational modes.[26] Thus, similarly to the above-discussed vibrational mode-specific studies, we can investigate the initial rotational mode specificity of polyatomic chemical reactions. Such studies were performed for $H_2O^+ + H_2/D_2$,[28,29] $H/F/Cl + H_2O$,[30–32] $H/Cl/O + CHD_3$,[26,33–35] and the $F^- + CH_3F/CH_3Cl/CH_3I$[36,37] considering systems up to six atoms.

Besides the investigation of the initial state dependence of the reactivity, one is also interested in following the energy transfer from reactants to products. Most of the theoretical and experimental studies can only determine the translational and internal energy, or in some cases the total vibrational and rotational energy, of the products, however, little is known about the mode-specific energy distributions in the case of a polyatomic product. Experimentally, Liu and co-workers could probe specific vibrational states of the methyl ($CH_3$, $CD_3$, $CHD_2$, *etc.*) products of the atom + methane reactions.[14,16,21] Theoretically, Corchado and Espinosa-García[38] as well as Czakó and Bowman[17] developed mode-specific product vibrational analysis methods using a projection of the final coordinates and velocities of quasi-classical trajectories onto the normal coordinate space. However, classically the molecular vibrations are not quantized and rounding the classical actions to integer numbers may result in unphysical vibrational states. Bonnet and Rayez[39,40] proposed the so-called Gaussian binning (GB) method, which assigns a weight for each reactive trajectory, thereby incorporating some quantum effect into the QCT product analysis. The computational cost of GB, however, scales exponentially with the number of the vibrational modes, thus the original GB algorithm was found impractical for polyatomic products. To solve this problem, in 2009 Czakó and Bowman[17] proposed the one-dimensional GB (1GB) method,[17,41] which is efficient even for large product molecules. 1GB was first employed for the $F + CHD_3 (\nu_1 = 0, 1) \rightarrow HF/DF + CD_3/CHD_2$ reactions[17] and later many applications by different groups showed its usefulness.[42–56]

The early mode-specific studies focused on neutral systems and theoretically usually six or less atoms could be treated. Following some early work of Hennig and Schmatz[57–59] on the $X^- + CH_3Y$ systems, where X and Y are halogens, our group started to investigate the mode-specific dynamics of bimolecular nucleophilic substitution ($S_N2$) reactions.[60] In 2016 Szabó and Czakó in collaboration with the Guo and Yang groups reported vibrational mode-specific wave packet dynamics computations for the $F^- + CH_3Cl$ $S_N2$ reaction using a 6-dimensional model and a high-level *ab initio* PES.[60] In 2018 an experimental-theoretical collaboration between the Wester, Guo, and Czakó groups found that CH stretching excitation is a spectator in the $F^- + CH_3I$ $S_N2$ reaction, whereas enhances the proton-transfer channel.[61] Our analytical PESs were also utilized in mode-specific quantum dynamics computations for $S_N2$ reactions by Wang and co-workers.[62,63]

Moving beyond six-atom systems applying first-principles theory is challenging because of the high-dimensionality of the PES.[64] Nevertheless, several post-six-atom reactions were studied recently by analytical PES-based or direct dynamics approaches, and for some of them even mode-specific computations were also performed.[65–102] Espinosa-García and co-workers[77,78] and/or our group[90,91,93] investigated the mode-specificity in the reactions of ethane ($C_2H_6$) with H, F, Cl, and OH, while Lu and Li[82] studied the $F + CH_3OH$ reaction. We also reported mode-specific computations for $HBr/HI + C_2H_5$,[96–98] $CH_2OO + NH_3$[99] and post-six-atomic ion–molecule reactions, such as $OH^- + CH_3I$[102] and $F^- + CH_3CH_2Cl$.[54]

In the present Perspective article, we focus on our most recent first-principles mode-specific dynamics studies of the $F/Cl/OH + C_2H_6$,[90,91,93] $HBr/HI + C_2H_5$,[96–98] $OH^- + CH_3I$,[102] and $F^- + CH_3CH_2Cl$[54] reactions, covering both neutral and ionic systems with 7–10 atoms. Our theoretical approach is based on (1) automated *ab initio* analytical PES development utilizing our Robosurfer program system[103] interfaced with the Molpro electronic structure package[104,105] and the permutationally-invariant polynomial fitting codes,[106,107] as well as (2) QCT simulations using the new PESs. A graphical overview of the first-principles mode-specific reaction dynamics approach is presented in Fig. 1. In the next sections we describe how initial vibrational and rotational excitations affect the reactivity and the product energy release, while we also show how to perform mode-specific product analysis and demonstrate the utility of the 1GB approach. The review of these recent applications may set new directions for future mode-specific investigations for complex chemical systems.

## II. Vibrational mode specificity

For 4–6-atomic reactions initial-vibrational-state-specific reactivity can be studied using full- or reduced-dimensional quantum dynamics methods (see Fig. 1) as many examples on $X + H_2O/NH_3/CH_4$, [X = H, F, Cl] *etc.* show in the literature.[6,9,10,19,33,108,109] For larger systems the QCT approach provides an efficient tool to study mode-specific reactivity (see also Fig. 1), where the *N*-atomic

**15820** | *Phys. Chem. Chem. Phys.*, 2024, **26**, 15818–15830

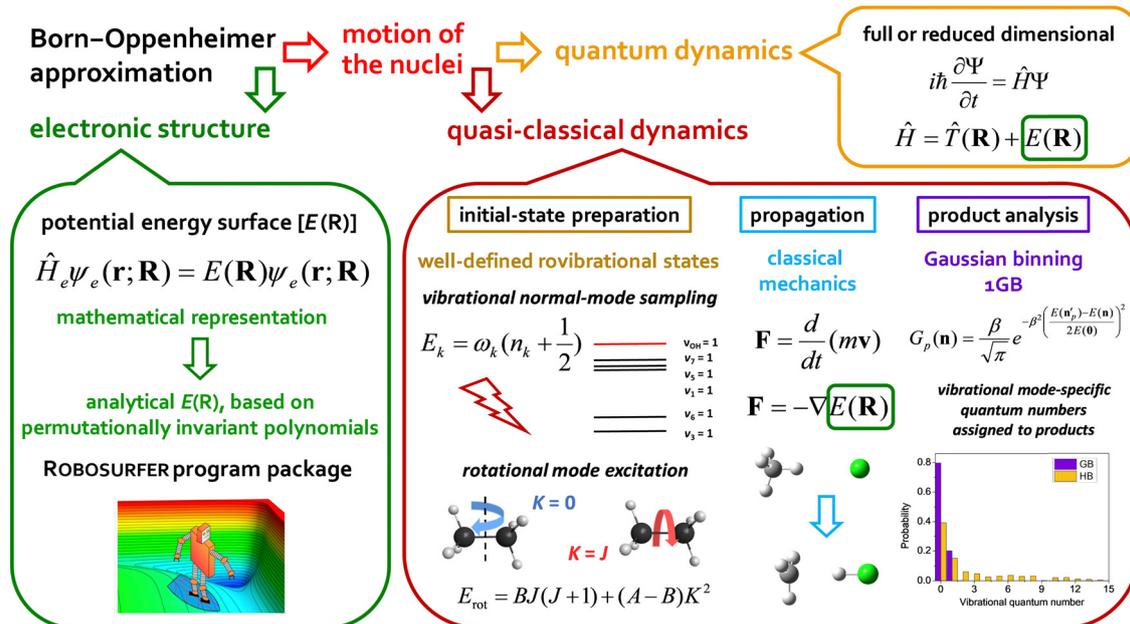This journal is © the Owner Societies 2024

**Fig. 1** Graphical representation of the first-principles mode-specific reaction dynamics approach.

non-linear (linear) reactants can be prepared in any vibrational state characterized by quantum numbers $(n_1, n_2, \ldots, n_{3N-6(5)})$ by selecting normal coordinates $(Q_k)$ and momenta $(P_k)$ as[110]

$$Q_k = \frac{\sqrt{2E_k}}{\omega_k}\cos(2\pi R_k) \quad k = 1, 2, \ldots, 3N - 6(5) \quad (1)$$

$$P_k = \sqrt{2E_k}\sin(2\pi R_k) \quad k = 1, 2, \ldots, 3N - 6(5), \quad (2)$$

where $R_k$ is a uniform random number between 0 and 1, $\omega_k$ denotes the harmonic frequencies, and the energy of each mode can be obtained *via* the quantum expression $E_k = (n_k + 1/2)\omega_k$. We applied the QCT method for several mode-specific studies on post-six-atom reactions[54,90,91,93,96–99,102] and below we highlight our representative results.

Fig. 2 shows the potential energy profiles of the valence-isoelectronic $X + C_2H_6 \rightarrow HX + C_2H_5$ [X = F, Cl, OH] reactions.[83,84,92] In the case of X = F, the reaction is highly exothermic with a slightly submerged very reactant-like transition state (TS). For X = OH the exothermicity is about half of that of the X = F reaction, and a classical (adiabatic) barrier with 4.0 (2.1) kcal mol$^{-1}$ height and a reactant-like TS structure emerge. The vibrationally-adiabatic reaction pathway of Cl + C$_2$H$_6$ is exothermic ($-3.1$ kcal mol$^{-1}$) and has a submerged slightly-late barrier ($-2.1$ kcal mol$^{-1}$), whereas classically the reaction becomes slightly endothermic (2.0 kcal mol$^{-1}$) with a positive barrier height (2.2 kcal mol$^{-1}$). We investigated the mode-specific reactivity of these $X + C_2H_6$ reactions[90,91,93] considering singly-excited initial vibrational modes as indicated in Fig. 2.

One of the main concerns in mode-specific reaction dynamics is the intramolecular vibrational-energy redistribution (IVR) prior to collision, which may undermine the mode-specific effects. We examined IVR in ethane by computing the
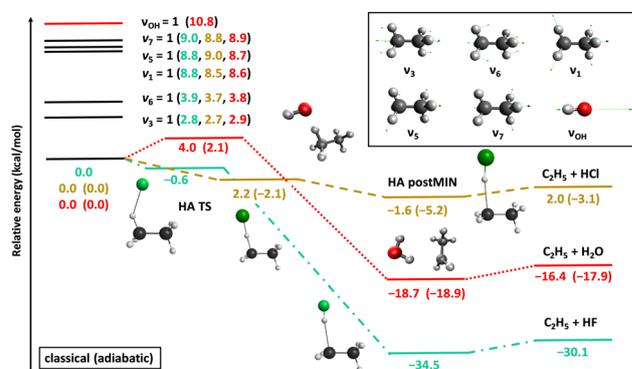


**Fig. 2** Schematic potential energy surfaces of the $X + C_2H_6$ [X = F, Cl, OH] hydrogen-abstraction reactions showing the stationary-point structures and their classical (adiabatic) relative energies corresponding to the analytical PESs,[83,84,92] as well as selected normal modes and singly-excited vibrational levels of the reactants.[90,91,93]

time evolution of its mode-specific energies[90] using the normal mode analysis technique[48] developed for product analysis (see details in Section IV). Fig. 3 shows the mode energies of the ground-state ($v = 0$), CH$_3$-deformation-excited ($v_6 = 1$), and symmetric-CH-stretching-excited ($v_1 = 1$) C$_2$H$_6$ as a function of time prior to collision. For $v = 0$ quantum mechanically no IVR can occur, however, classically the energy may flow from the high-frequency modes to the low-frequency ones. As Fig. 3 shows this classical "IVR" occurs within a few hundred femtoseconds, nevertheless, some mode-specific character of the energy distribution remains until the reactants collide, which usually happens in the 150–650 fs time range in our simulations. If the reactant is excited, IVR can occur even quantum mechanically/experimentally. The $v_6 = 1$ state is a good example, where IVR is not significant, whereas the $v_1 = 1$ state loses its CH stretching-

This journal is © the Owner Societies 2024

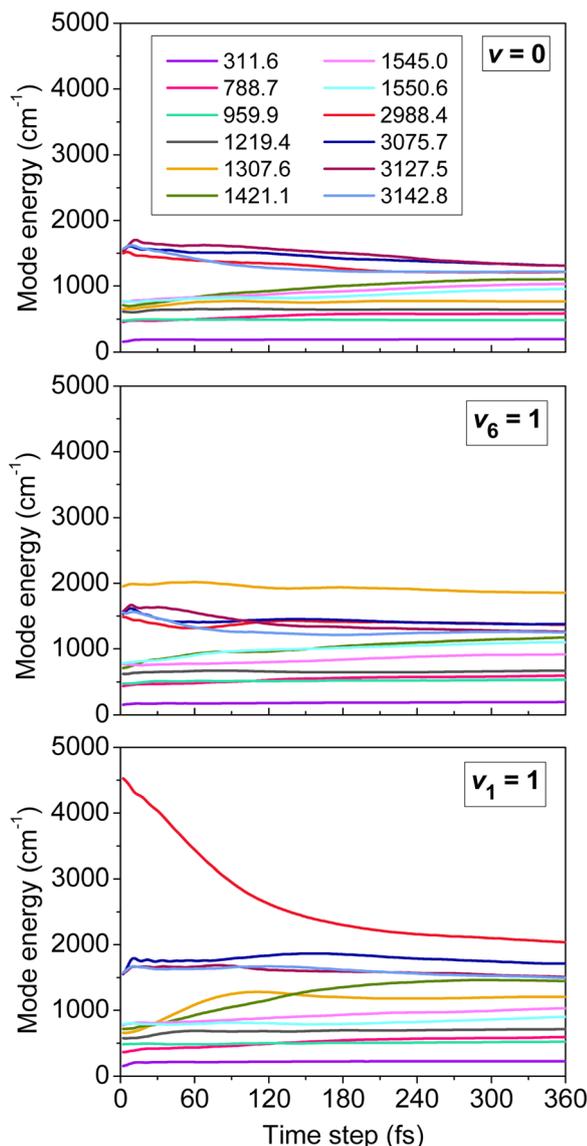*Phys. Chem. Chem. Phys.*, 2024, **26**, 15818–15830 | **15821**

Fig. 3 Mode-specific vibrational energies of a non-interacting $C_2H_6$ molecule as a function of time corresponding to the ground ($v = 0$), $CH_3$ deformation-excited ($v_6 = 1$), and symmetric CH stretching-excited ($v_1 = 1$) states.[90] The modes are labeled by their harmonic frequencies (in $cm^{-1}$).

excited character as the reactants approach each other. Here QCT may overestimate the speed of IVR, because the effect may come from both the artifacts of classical mechanics and the real IVR, which is a fundamental process in vibrationally excited molecules. Nevertheless, the reactant retains some CH stretching-excited character in the entrance channel, suggesting mode specificity in the X + $C_2H_6$ reactions.

Initial-vibrational-state-specific cross sections of the X + $C_2H_6$ [F, Cl, OH] reactions as a function of collision and total energy are shown in Fig. 4. The cross sections increase with collision energy and the shape of the excitation functions (cross sections *vs.* collision energy) is similar for X = F and OH. The higher reactivity of F + $C_2H_6$ is expected because of its lower (negative) barrier and higher exothermicty as well as the

spherical character of one of the reactants (F), while the reaction of OH requires a special orientation. For both X = F and OH the excitations of the CH stretching modes enhance the reactivity the most efficiently, as expected as a CH bond breaks during the hydrogen-abstraction processes. The other modes either do not have significant effect on the reactivity or slightly inhibit the reaction, like CC stretching ($v_3$). Considering the total energy (collision energy and vibrational energy) dependence of the reactivity, in the case of the F + $C_2H_6$ reaction one can clearly see that at a given total energy the ground-state reaction has the highest reactivity, which means that it is advantageous to invest the energy into translational motion, in accord with the Polanyi rules in the case of an early-barrier reaction. However, for the also early-barrier OH + $C_2H_6$ reaction the picture is less obvious: except $v_3$ and $v_{OH}$ excitations, many modes promote the reaction similarly or more efficiently than translational energy, in contradiction with the Polanyi rules. This finding is not completely surprising, because, as we mentioned earlier, the Polanyi rules were formulated for atom + diatom reactions and there is no guarantee that these rules always remain valid for polyatomic processes. In fact, violations of the Polanyi rules have been found for several systems such as, for example, F + $H_2O$,[111] OH + $H_2S$,[112] and Cl + $CHD_3$.[14,18] The cross sections of the Cl + $C_2H_6$ reaction decrease with increasing collision energy, because the adiabatic reaction pathway is clearly submerged. Similarly to the X = F and OH cases, CH stretching excitations promote the reactivity the most efficiently, whereas the $v_6$ mode has only a minor enhancement and $v_3$ excitation has negligible effect or causes a slight inhibition at the lowest collision energies. Since translational energy does not activate the reaction, at a given total energy the vibrationally-excited reactions have higher reactivity, in accord with the Polanyi rules in the case of a late-barrier reaction.

In 2013 Jiang and Guo[113] proposed a sudden vector projection (SVP) method as a generalization of the Polanyi rules. The SVP approach calculates the overlap between the normal modes of the reactant with the imaginary mode of the TS. SVP has been proven useful in many applications,[90,114,115] though it has limitations: it (1) works well only for direct processes, (2) cannot account for IVR, (3) cannot describe inhibition, and (4) does not consider collision energy dependence. We applied SVP for the Cl + $C_2H_6$ reaction and found good overall agreement with the QCT results, for example, the largest SVP values were obtained for the CH stretching modes.[90]

In Fig. 5 we show initial-state-dependent product internal and relative translational energy distributions for the X + $C_2H_6 \rightarrow HX + C_2H_5$ [X = F, Cl, OH] reactions. For all three reactions the translational energy distributions show virtually no initial vibrational state dependence, suggesting that the reactants' vibrational excitation energy transfers into the internal degrees of freedom of the products. For X = F and Cl, the internal energy distributions of the $C_2H_5$ products blue-shift approximately with the amount of the initial vibrational excitation energy, showing that the major part of the excess vibrational energy remains in the polyatomic product. For X = OH mode-specific effects are also seen in the product internal
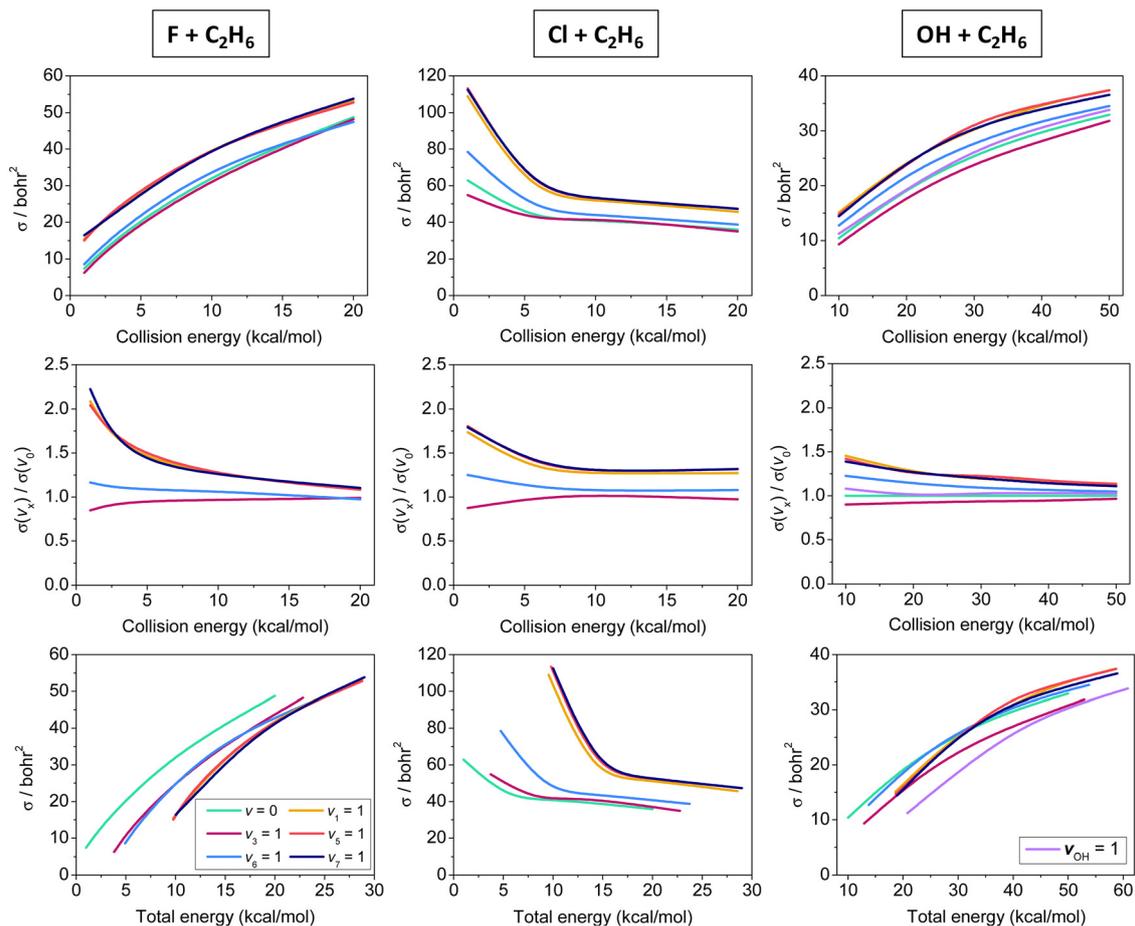
**Fig. 4** Vibrational mode-specific cross sections and their ratios as a function of collision energy and cross sections as a function of total energy for the X + C$_2$H$_6$ [X = F, Cl, OH] hydrogen-abstraction reactions.[90,91,93]
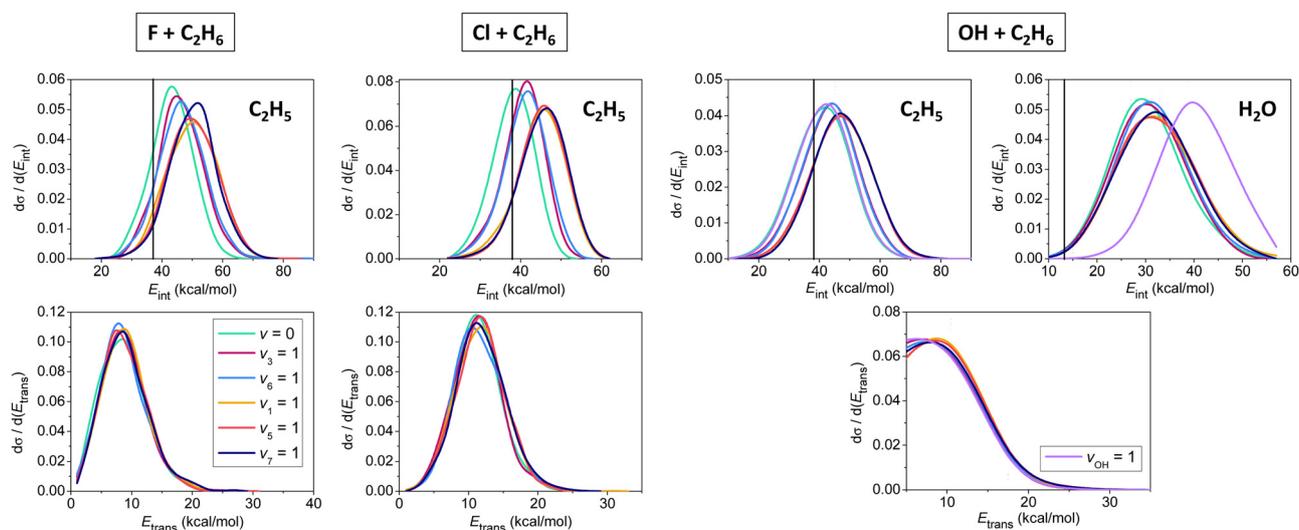


**Fig. 5** Normalized vibrational mode-specific product internal (upper panels) and relative translational (lower panels) energy distributions for the X + C$_2$H$_6$ [X = F, Cl, OH] hydrogen-abstraction reactions at a collision energy of 10 kcal mol$^{-1}$.[90,91,93] Vertical lines show the zero-point energies of the products.
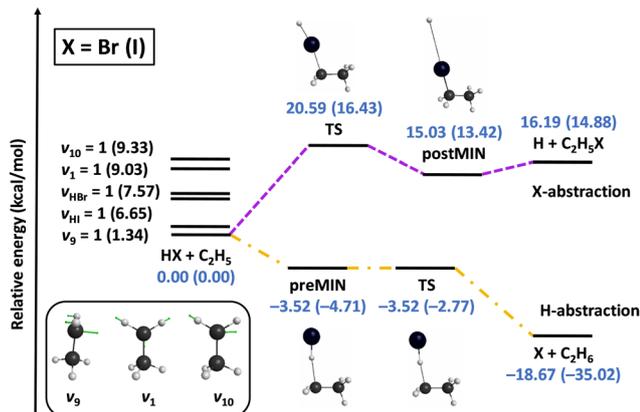
This journal is © the Owner Societies 2024

*Phys. Chem. Chem. Phys.*, 2024, **26**, 15818–15830 | **15823**

**Fig. 6** Schematic potential energy surfaces of the HX + $C_2H_5$ [X = Br, I] reactions showing the stationary-point structures and their classical relative energies corresponding to the analytical PESs, as well as selected normal modes and singly-excited vibrational levels of the reactants.[98]

energy distributions. CH stretching excitation energy mainly remains in the $C_2H_5$ product, whereas OH stretching becomes a spectator mode, exciting the $H_2O$ product as the extents of the blue-shifts show in Fig. 5. It is also evident that the $H_2O$ products are formed vibrationally excitedly, in accord with the early-barrier nature of the OH + $C_2H_6$ reaction.

We also investigated the mode specificity in the HX + $C_2H_5$ [X = Br, I] reactions,[96–98] whose schematic potentials are shown

in Fig. 6. In both cases the main reaction pathway is hydrogen abstraction, which goes through submerged pre-reaction complexes and TSs leading to the X + $C_2H_6$ products. For both X = Br and I hydrogen abstraction is exothermic, and the exothermicity is about twice as larger in the case of X = I due to the lower dissociation energy of HI relative to HBr. Besides hydrogen abstraction, halogen abstraction can also occur *via* endothermic pathways resulting in H + $C_2H_5X$ products, as also shown in Fig. 6. Here the energetics for X = Br and I are similar, because the HBr *vs.* HI and C–Br *vs.* C–I bond-energy differences are close to each other.

The mode-specific cross sections of the HX + $C_2H_5$ [X = Br, I] H- and X-abstraction reactions as a function of collision energy are shown in Fig. 7. At low collision energies H abstraction dominates, but around 30–40 kcal mol$^{-1}$ the X-abstraction channel opens, and at higher collision energies the two channels become competitive. HX vibrational excitation enhances both abstraction channels, but the promotion effect is much more substantial for X abstraction. As a HX bond breaks in both abstraction processes, we may not expect significant impact on reactivity upon $C_2H_5$ excitations. This is true for the X-abstraction channel, but for H abstraction clear inhibition effects are found, especially in the case of the excitation of the $CH_2$ wagging ($v_9$) mode inducing steric hindrance.

Besides the neutral systems, we have also performed mode-specific investigations for ion–molecule reactions.[54,60,61,102]
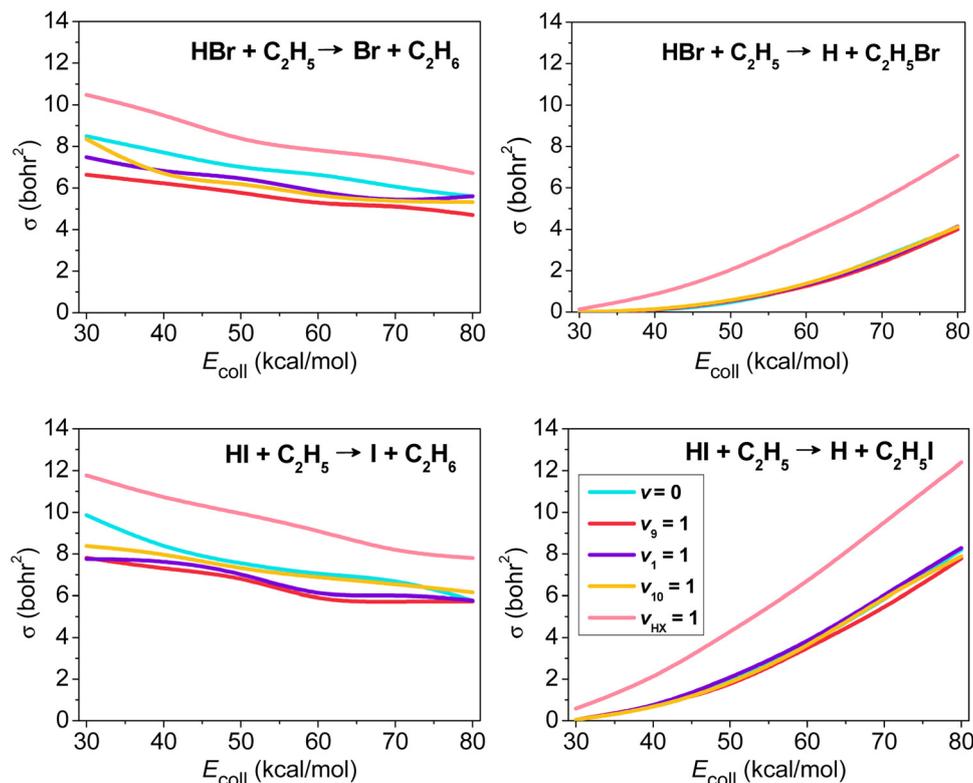


**Fig. 7** Vibrational mode-specific cross sections as a function of collision energy for the hydrogen- and halogen-abstraction channels of the HX + $C_2H_5$ [X = Br, I] reactions.[98]

**15824** | *Phys. Chem. Chem. Phys.*, 2024, **26**, 15818–15830
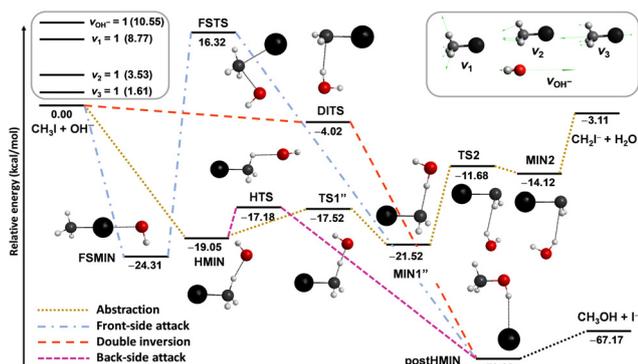
This journal is © the Owner Societies 2024

**Fig. 8** Simplified schematic potential energy surface of the $OH^- + CH_3I$ reaction showing the stationary-point structures and their classical relative energies corresponding to the analytical PES[87] along the different reaction pathways, as well as selected normal modes and singly-excited vibrational levels of the reactants.[102]

Here we highlight our most recent results on the $OH^- + CH_3I$ system.[102] Its main reaction channel is the $S_N2$, which is highly exothermic and may proceed *via* the submerged back-side attack Walden-inversion, the also slightly submerged double-inversion or the high-barrier front-side attack pathway, as shown in Fig. 8. In addition to the $S_N2$ channel, there is a less exothermic proton-abstraction channel, which leads to the $H_2O + CH_2I^-$ products *via* an also submerged reaction path. It is interesting to see how the excitation of selected vibrational modes, CI stretching ($v_3$), umbrella ($v_2$), symmetric CH stretching ($v_1$), and OH stretching (see Fig. 8), affects the reactivity of this barrier-less reaction.

The mode-specific cross sections for the $S_N2$ and proton-abstraction channels of the $OH^- + CH_3I$ reaction are shown in Fig. 9. As expected in the case of barrier-less exothermic reactions, the reactivity decreases with increasing collision energy for both channels. However, it is somewhat surprising that the thermodynamically favored $S_N2$ channel has significantly lower reactivity than proton abstraction. This may be explained by the dominance of H-bonded complex and TS formation in the entrance channel (see Fig. 8), which favors proton abstraction over the deep product well of the substitution pathway. The $S_N2$ channel is clearly enhanced by the excitation of the CI stretching and umbrella modes, as expected, because the CI bond breaks and the $CH_3$ group inverts *via* an umbrella motion during Walden inversion, which is the dominant $S_N2$ pathway. The CH and OH stretchings have less effect on the $S_N2$ reactivity, they mostly behave as spectators in the substitution process. In the case of proton abstraction, the CH stretching excitation promotes the reaction the most efficiently, as expected, since a CH bond breaks in the abstraction process. The umbrella motion also helps the proton transfer, whereas the CI and OH stretching excitations have negligible effects on the abstraction reactivity. The total energy dependence of the mode-specific reactivity is tricky, because extra collision energy significantly decreases the reactivity, therefore, at a given total energy it is the most advantageous if a major part of the energy is in vibration and a minor part is

in translation. Thus, the highest-energy vibrational modes (CH and OH stretchings) show the most substantial enhancement effects, however, in some cases, due to an indirect reason, *i.e.*, less energy remains for translation, which results in higher reactivity. The CH stretching effects were also studied experimentally by Wester and co-workers[116,117] for the iso-electronic $F^- + CH_3I$ reaction, and their main observations are in agreement with the present theoretical results for the $OH^- + CH_3I$ system. For the $OH^- + CH_3I$ reaction reduced-dimensional quantum dynamics computations were also carried out by Rao and Wang[63] using our PES.[87] The promotion effect of the CI stretching excitation was found in the quantum study as well, however, in the reduced-dimensional model the umbrella excitation unexpectedly hindered the $S_N2$ reactivity. This inhibition effect may be an artifact of the model of Rao and Wang as the Palma-Clary-type 6-dimensional quantum computations found promotion effects upon umbrella excitation in the case of the $F^- + CH_3Cl$ reaction.[60] These findings may motivate future experiments for umbrella-excited $S_N2$ reactions.

## III. Rotational mode specificity

In QCT simulations one can also prepare the reactants in a specific rotational state (see Fig. 1). In the case of a symmetric top molecule the initial rotational angular momentum vector, $\mathbf{j}^{PAS} = (j_x^{PAS}, j_y^{PAS}, j_z^{PAS})$, corresponding to quantum numbers $J$ and $K$ can be obtained *via* the following expressions in the principal axis system (PAS):

$$j = \sqrt{J(J+1)} \tag{3}$$

$$j_z^{PAS} = K \tag{4}$$

$$j_x^{PAS} = (j^2 - K^2)^{1/2} \sin 2\pi R \tag{5}$$

$$j_y^{PAS} = (j^2 - K^2)^{1/2} \cos 2\pi R \tag{6}$$

where $R \in [0, 1]$ is a uniform random real number. Then, the $\mathbf{j}^{PAS}$ vector is transformed to the space-fixed Cartesian space and the obtained angular momentum is set by standard modification of the velocities.[110] Note that eqn (4)–(6) are given for oblate-type rotors, for prolate symmetric tops $j_x^{PAS} = K$.

We studied the rotational-mode-specific reactivity of several symmetric top molecules such as $CHD_3$,[26,35] $CH_3X$ [X = F, Cl, I],[36,37] and $C_2H_6$.[118] Here we focus on our most recent results on the $Cl + C_2H_6(v = 0, JK)$ reaction.[118] In Fig. 10 we show the $JK$-specific cross sections as a function of collision energy for the $Cl + C_2H_6$ reaction considering two limiting cases, which correspond to tumbling ($K = 0$) and spinning ($K = J$) rotation. As seen, rotational excitation usually enhances the reactivity and the effects of the spinning excitations are clearly more significant than the corresponding tumbling enhancements. This finding can be explained by the facts that the $K = 0$ states have much smaller energies than the corresponding $K = J$ states (see Fig. 10), and the

This journal is © the Owner Societies 2024

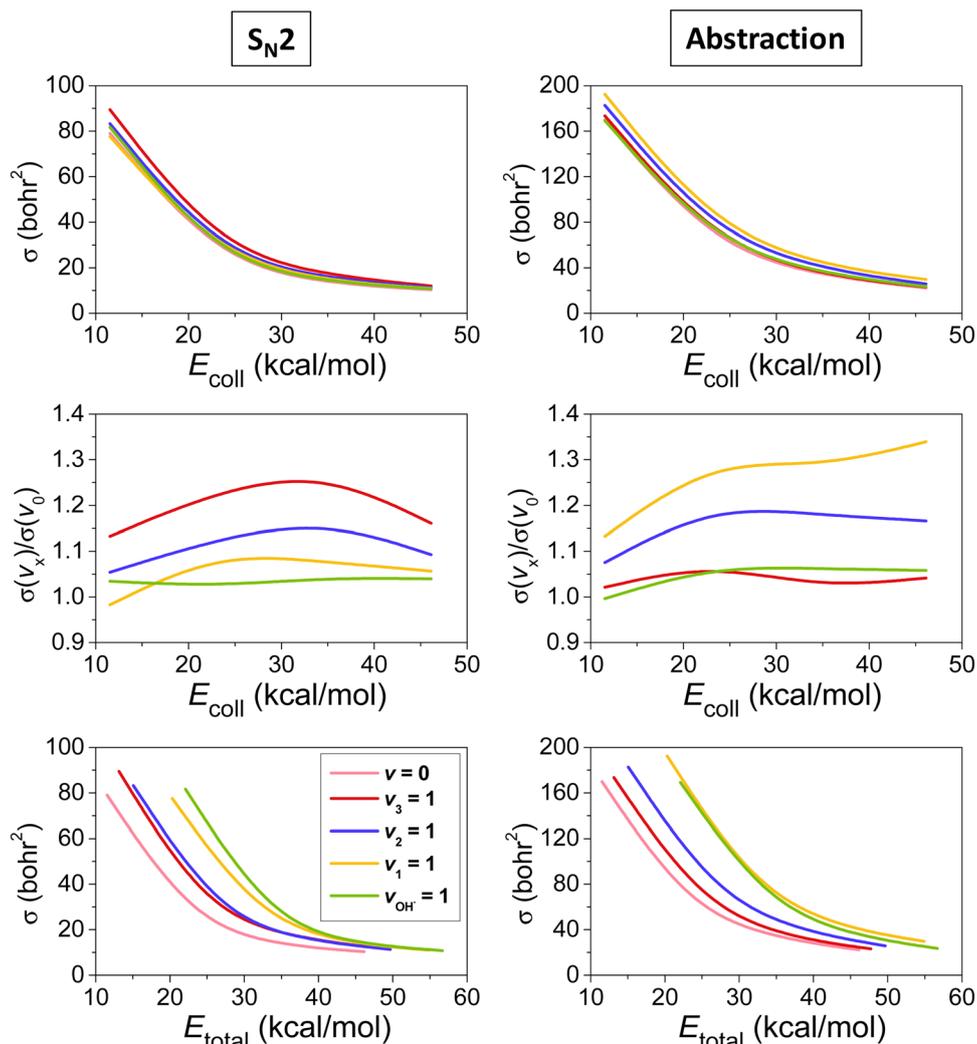*Phys. Chem. Chem. Phys.*, 2024, **26**, 15818–15830 | **15825**

Fig. 9 Vibrational mode-specific cross sections and their ratios as a function of collision energy and cross sections as a function of total energy for the $S_N2$ and proton-abstraction channels of the $OH^- + CH_3I$ reaction.[102]
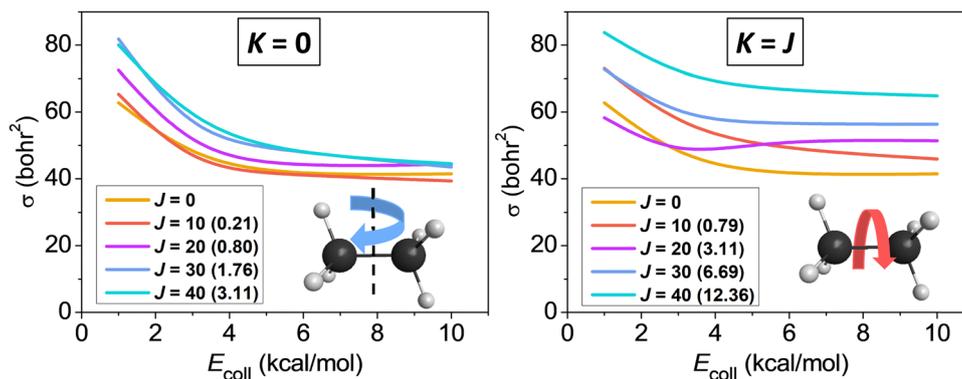


Fig. 10 Rotational-state-specific cross sections as a function of collision energy for the $Cl + C_2H_6(v = 0, JK)$ reaction.[118] The rotational energies are given in parentheses in kcal mol$^{-1}$.

centrifugal force caused by the spinning excitation elongates the CH bonds thereby promoting their cleavage. We found similar spinning rotational effect in the proton-abstraction channel of the $F^- + CH_3I$ reaction.[37]

15826 | *Phys. Chem. Chem. Phys.*, 2024, **26**, 15818–15830

This journal is © the Owner Societies 2024

# IV. Mode-specific product vibrational distributions

Following the early work of Corchado and Espinosa-García,[38] we developed a normal mode analysis method to compute mode-specific product vibrational distributions from QCT simulations (see Fig. 1).[17,48] The key steps of the normal mode analysis approach are summarized below:

(1) We perform a normal mode analysis at the equilibrium structure of the product in the center of mass frame.

(2) We find the best overlap between the actual geometry of the product and its equilibrium structure by an exact Eckart transformation.[48,119]

(3) We project the Cartesian coordinates and velocities of the product to the normal mode space.

(4) We compute the energy for each normal mode using the quadratic harmonic expression for the potential.

(5) The mode-specific non-integer vibrational quantum numbers are determined from the mode energies using the quantum mechanical energy formula of a harmonic oscillator.
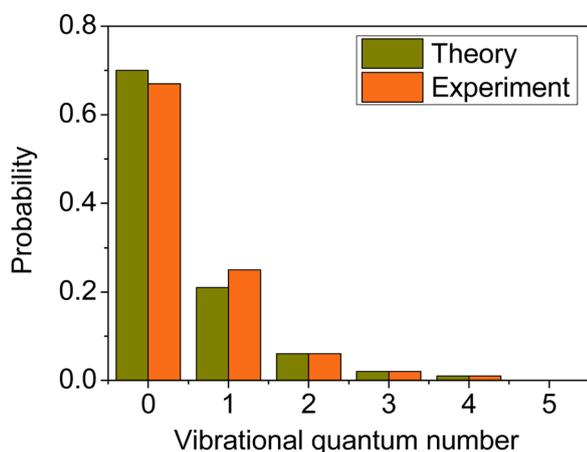
Then the integer quantum numbers are obtained by rounding the real values to the nearest integer.

The above analysis may provide unphysical vibrational states due to the rounding issue (rounding up may result in energetically not available states) and the breakdown of the normal mode analysis at highly distorted structures. To handle these issues, we proposed the 1GB method,[17,48] which assigns a weight for each product ($p$) as

$$G_p(\mathbf{n}) = \frac{\beta}{\sqrt{\pi}} e^{-\beta^2 \left( \frac{E(\mathbf{n}'_p) - E(\mathbf{n})}{2E(\mathbf{0})} \right)^2} \tag{7}$$

where $E(\mathbf{n})$ is the harmonic vibrational energy corresponding to the given state ($\mathbf{n}$), $E(\mathbf{0})$ is the harmonic zero-point energy, and $\beta$ is a fixed positive real parameter controlling the width of the Gaussian. $E(\mathbf{n}'_p)$ is the actual vibrational energy of the $p$th product, which should be computed using the velocities in the Cartesian space and the PES used in the QCT simulation. With these definitions 1GB solves both the rounding and normal mode analysis breakdown issues mentioned above. 1GB has been employed by several research groups for various systems with great success,[42–56] below we highlight our most recent results.

We computed the mode-specific vibrational distributions for the $H_2O$ product of the OH + $C_2H_6(v = 0)$ reaction[93] and we show the populations of the bending mode in Fig. 11. The computed mode-specific distributions allow comparison with the infrared chemiluminescence data measured by Butkovskaya and Setser.[120] As Fig. 11 shows, the agreement between theory[93] and experiment[120] is excellent. Both the computed and measured data show that $H_2O$ is mainly formed in the ground bending state ($\sim 70\%$), the one-quantum excitation has about 20–25% probability, and the populations of the overtones are small and decrease with increasing vibrational quanta. Here we did not use 1GB, because $H_2O$ does not have low-frequency torsional modes, which would compromise the normal mode analysis, and there are several open vibrational states, which makes the rounding issue less problematic. Note, that when we studied the dissociation dynamics of the water dimer, the use of 1GB was essential, because the $H_2O$ fragments could be



**Fig. 11** Comparison of the computed[93] (collision energy of 10 kcal mol$^{-1}$) and measured[120] bending mode specific vibrational distributions for the $H_2O$ product of the OH + $C_2H_6(v = 0)$ hydrogen-abstraction reaction.
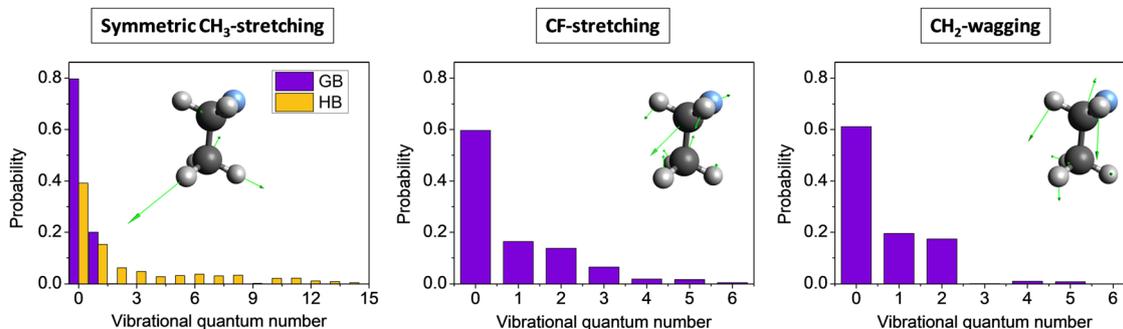


**Fig. 12** Symmetric $CH_3$-stretching, CF-stretching, and $CH_2$-wagging mode-specific vibrational distributions for the $CH_3CH_2F$ product of the $F^- + CH_3CH_2Cl(v = 0)$ $S_N2$ reaction obtained by histogram binning (HB, left panel) and Gaussian binning (GB, all panels) at a collision energy of 26.5 kcal mol$^{-1}$.[54]

This journal is © the Owner Societies 2024

*Phys. Chem. Chem. Phys.*, 2024, **26**, 15818–15830 | **15827**

formed in only two vibrational states.[42] In the case of OH + $C_2H_6$ Rangel et al.[86] also computed the mode-specific distributions for the $H_2O$ product using their PES-2020 and found similar populations as described above. They applied 1GB as well, and obtained qualitatively the same results as with standard binning.

Mode-specific vibrational distributions for selected modes of the $CH_3CH_2F$ product of the $F^- + CH_3CH_2Cl(v = 0)$ $S_N2$ reaction[54] are shown in Fig. 12. In the case of symmetric $CH_3$ stretching the standard histogram binning shows the dominance of the ground stretching state as expected, however, gives small populations up to and beyond 15 quanta, which is clearly unphysical. The reason behind this issue is the breakdown of the normal mode analysis due to the large amplitude torsional motion of the $CH_3$ group. The 1GB method solves this problem and provides non-zero populations for the ground (80%) and first-excited (20%) stretching states only, i.e., the unphysical small populations completely vanish. In the case of the CF-stretching and $CH_2$-wagging modes 1GB also shows that the ground state is the most populated ($\sim 60\%$), but excitations with one quantum ($\sim 20\%$) and two quanta ($\sim 20\%$) are also significant and small populations up to 5–6 quanta are found as well. This finding is in agreement with our chemical intuition as these two modes play an active role in the Walden inversion process.

## V. Summary and conclusions

We have reviewed the field of mode-specific reaction dynamics from our perspective, focusing on recent results for several neutral and ionic reactive systems beyond six atoms. The main general conclusions can be summarized as follows:

(1) IVR prior to collision can be monitored using the mode-specific product analysis method. Even if some IVR occurs, mode-specific dynamics can be obtained. Here we should mention that the timescale of an experiment may be longer than that of a QCT simulation. Furthermore, it is unclear which portion of IVR found in QCT simulations comes from a real effect and from the classical nature of the trajectories.

(2) Mode-specific effects can be obtained for barrier-less reactions, where the submerged TS can serve as a bottleneck for reactivity.

(3) The violation of the Polanyi rules is not unexpected in polyatomic processes.

(4) Rotational mode-specificity is a highly unexplored area of this field. Our computations show that specific types of rotations have different effects on the reactivity.

(5) In the case of multi-channel reactions different initial vibrational excitations may promote different channels, allowing the control of chemical processes.

(6) Excess vibrational energy usually shows up in product vibration, whereas the product translational energy is not affected.

(7) QCT simulations allow to compute mode-specific product vibrational distributions. To include some quantum spirit,

the 1GB method was proposed, which is essential if only few quantum states are available and/or the normal mode analysis fails due to high distortions of the product.

On one hand, the present perspective article shows that a lot of valuable knowledge accumulated in the field of mode-specific reaction dynamics thanks to the interplay of theory and experiment. On the other hand, there is a lot more to do, for example, it would be beneficial to have more experimental and/or quantum dynamics results for mode-specific product distributions, which could be compared with the QCT results. Hopefully the present subjective review will motivate us to move this field forward.

## Data availability

The data that support the findings of this study are available from the corresponding author upon reasonable request.

## Conflicts of interest

There are no conflicts of interest to declare.

## Acknowledgements

## References

1  J. C. Polanyi, Science, 1987, 236, 680.
2  G. C. Schatz, M. C. Colton and J. L. Grant, J. Phys. Chem., 1984, 88, 2971.
3  A. Sinha, M. C. Hsiao and F. F. Crim, J. Chem. Phys., 1990, 92, 6333.
4  R. B. Metz, J. D. Thoemke, J. M. Pfeiffer and F. F. Crim, J. Chem. Phys., 1993, 99, 1744.
5  M. J. Bronikowski, W. R. Simpson, B. Girard and R. N. Zare, J. Chem. Phys., 1991, 95, 8647.
6  D. H. Zhang and J. C. Light, J. Chem. Soc., Faraday Trans., 1997, 93, 691.
7  W. R. Simpson, T. P. Rakitzis, S. A. Kandel, T. Lev-On and R. N. Zare, J. Phys. Chem., 1996, 100, 7938.
8  J. C. Corchado, D. G. Truhlar and J. Espinosa-García, J. Chem. Phys., 2000, 112, 9375.
9  D. Y. Wang and J. M. Bowman, J. Chem. Phys., 2001, 115, 2055.

15828 | Phys. Chem. Chem. Phys., 2024, 26, 15818–15830

This journal is © the Owner Societies 2024

10 M. Yang, D. H. Zhang and S.-Y. Lee, *J. Chem. Phys.*, 2002, **117**, 9539.

11 S. Yoon, S. Henton, A. N. Zivkovic and F. F. Crim, *J. Chem. Phys.*, 2002, **116**, 10744.

12 Z. Xie, J. M. Bowman and X. Zhang, *J. Chem. Phys.*, 2006, **125**, 133120.

13 J. Sansón, J. C. Corchado, C. Rangel and J. Espinosa-García, *J. Phys. Chem. A*, 2006, **110**, 9568.

14 S. Yan, Y.-T. Wu, B. Zhang, X.-F. Yue and K. Liu, *Science*, 2007, **316**, 1723.

15 J. Espinosa-García, *J. Chem. Phys.*, 2009, **130**, 054305.

16 W. Zhang, H. Kawamata and K. Liu, *Science*, 2009, **325**, 303.

17 G. Czakó and J. M. Bowman, *J. Chem. Phys.*, 2009, **131**, 244302.

18 G. Czakó and J. M. Bowman, *Science*, 2011, **334**, 343.

19 Z. Zhang, Y. Zhou, D. H. Zhang, G. Czakó and J. M. Bowman, *J. Phys. Chem. Lett.*, 2012, **3**, 3416.

20 G. Czakó and J. M. Bowman, *J. Phys. Chem. A*, 2014, **118**, 2839.

21 J. J. Lin, J. Zhou, W. Shiu and K. Liu, *Science*, 2003, **300**, 966.

22 G. Czakó and J. M. Bowman, *J. Am. Chem. Soc.*, 2009, **131**, 17534.

23 G. Czakó, Q. Shuai, K. Liu and J. M. Bowman, *J. Chem. Phys.*, 2010, **133**, 131101.

24 B. Zhang, K. Liu and G. Czakó, *J. Phys. Chem. A*, 2015, **119**, 7190.

25 H. Pan, F. Wang, G. Czakó and K. Liu, *Nat. Chem.*, 2017, **9**, 1175.

26 R. Liu, F. Wang, B. Jiang, G. Czakó, M. Yang, K. Liu and H. Guo, *J. Chem. Phys.*, 2014, **141**, 074310.

27 R. Liu, M. Yang, G. Czakó, J. M. Bowman, J. Li and H. Guo, *J. Phys. Chem. Lett.*, 2012, **3**, 3776.

28 Y. Xu, B. Xiong, Y.-C. Chang and C. Y. Ng, *J. Chem. Phys.*, 2012, **137**, 241101.

29 A. Li, Y. Li, H. Guo, K.-C. Lau, Y. Xu, B. Xiong, Y.-C. Chang and C. Y. Ng, *J. Chem. Phys.*, 2014, **140**, 011102.

30 B. Jiang, D. Xie and H. Guo, *J. Chem. Phys.*, 2011, **135**, 084112.

31 B. Jiang, J. Li and H. Guo, *J. Chem. Phys.*, 2014, **140**, 034112.

32 H. Song and H. Guo, *J. Phys. Chem. A*, 2015, **119**, 6188.

33 Z. Zhang and D. H. Zhang, *J. Chem. Phys.*, 2014, **141**, 144309.

34 F. Wang, H. Pan and K. Liu, *J. Phys. Chem. A*, 2015, **119**, 11983.

35 G. Czakó, *J. Phys. Chem. A*, 2014, **118**, 11683.

36 I. Szabó and G. Czakó, *J. Phys. Chem. A*, 2015, **119**, 12231.

37 P. Papp and G. Czakó, *J. Phys. Chem. A*, 2020, **124**, 8943.

38 J. C. Corchado and J. Espinosa-García, *Phys. Chem. Chem. Phys.*, 2009, **11**, 10157.

39 L. Bonnet and J. C. Rayez, *Chem. Phys. Lett.*, 1997, **277**, 183.

40 L. Bonnet and J. C. Rayez, *Chem. Phys. Lett.*, 2004, **397**, 106.

41 L. Bonnet and J. Espinosa-García, *J. Chem. Phys.*, 2010, **133**, 164108.

42 G. Czakó, Y. Wang and J. M. Bowman, *J. Chem. Phys.*, 2011, **135**, 151102.

43 J. D. Sierra, L. Bonnet and M. González, *J. Phys. Chem. A*, 2011, **115**, 7413.

44 L. Bonnet, J. Espinosa-García, J. C. Corchado, S. Liu and D. H. Zhang, *Chem. Phys. Lett.*, 2011, **516**, 137.

45 E. García, J. C. Corchado and J. Espinosa-García, *J. Comput. Theor. Chem.*, 2012, **990**, 47.

46 G. Czakó and J. M. Bowman, *J. Chem. Phys.*, 2012, **136**, 044307.

47 G. Czakó and J. M. Bowman, *Proc. Natl. Acad. Sci. U. S. A.*, 2012, **109**, 7997.

48 G. Czakó, *J. Phys. Chem. A*, 2012, **116**, 7467.

49 R. Conte, B. Fu, E. Kamarchik and J. M. Bowman, *J. Chem. Phys.*, 2013, **139**, 044104.

50 L. Bonnet and J. Espinosa-Garcia, *Phys. Chem. Chem. Phys.*, 2017, **19**, 20267.

51 Y. Zhu, L. Tian, H. Song and M. Yang, *J. Phys. Chem. A*, 2020, **124**, 6794.

52 L. Zhang, J. Chen and B. Jiang, *J. Phys. Chem. C*, 2021, **125**, 4995.

53 M. Braunstein, L. Bonnet and O. Roncero, *Phys. Chem. Chem. Phys.*, 2022, **24**, 5489.

54 V. Tajti and G. Czakó, *Phys. Chem. Chem. Phys.*, 2022, **24**, 8166.

55 Q. Yu and J. M. Bowman, *Nat. Commun.*, 2023, **14**, 3527.

56 J. Li, Z. Tu, H. Xiang, Y. Li and H. Song, *Phys. Chem. Chem. Phys.*, 2023, **25**, 20997.

57 C. Hennig and S. Schmatz, *J. Chem. Phys.*, 2004, **121**, 220.

58 C. Hennig and S. Schmatz, *J. Chem. Phys.*, 2005, **122**, 234307.

59 C. Hennig and S. Schmatz, *Chem. Phys. Lett.*, 2007, **446**, 250.

60 Y. Wang, H. Song, I. Szabó, G. Czakó, H. Guo and M. Yang, *J. Phys. Chem. Lett.*, 2016, 7, 3322.

61 M. Stei, E. Carrascosa, A. Dörfler, J. Meyer, B. Olasz, G. Czakó, A. Li, H. Guo and R. Wester, *Sci. Adv.*, 2018, **4**, eaas9544.

62 Y. Li, Y. Wang and D. Wang, *J. Phys. Chem. A*, 2017, **121**, 2773.

63 S. Rao and D. Wang, *Chin. J. Chem. Phys.*, 2023, **36**, 169.

64 G. Czakó, T. Győri, D. Papp, V. Tajti and D. A. Tasi, *J. Phys. Chem. A*, 2021, **125**, 2385.

65 B. Fu, Y.-C. Han, J. M. Bowman, L. Angelucci, N. Balucani, F. Leonori and P. Casavecchia, *Proc. Natl. Acad. Sci. U. S. A.*, 2012, **109**, 9733.

66 X. Shan and D. C. Clary, *Phys. Chem. Chem. Phys.*, 2013, **15**, 1222.

67 J. Li and H. Guo, *J. Chem. Phys.*, 2015, **143**, 221103.

68 B. Hornung, T. J. Preston, S. Pandit, J. N. Harvey and A. J. Orr-Ewing, *J. Phys. Chem. A*, 2015, **119**, 9452.

69 J. Zhang, L. Yang, J. Xie and W. L. Hase, *J. Phys. Chem. Lett.*, 2016, 7, 660.

70 B. Fu, X. Shan, D. H. Zhang and D. C. Clary, *Chem. Soc. Rev.*, 2017, **46**, 7625.

71 M. L. Weichman, J. A. DeVine, M. C. Babin, J. Li, L. Guo, J. Ma, H. Guo and D. M. Neumark, *Nat. Chem.*, 2017, **9**, 950.

72 E. Carrascosa, J. Meyer, J. Zhang, M. Stei, T. Michaelsen, W. L. Hase, L. Yang and R. Wester, *Nat. Commun.*, 2017, **8**, 25.

This journal is © the Owner Societies 2024

*Phys. Chem. Chem. Phys.*, 2024, **26**, 15818–15830 | **15829**

73 S. Pandit, B. Hornung, G. T. Dunning, T. J. Preston, K. Brazener and A. J. Orr-Ewing, *Phys. Chem. Chem. Phys.*, 2017, **19**, 1614.

74 O. Roncero, A. Zanchet and A. Aguado, *Phys. Chem. Chem. Phys.*, 2018, **20**, 25951.

75 C. Rangel and J. Espinosa-Garcia, *Phys. Chem. Chem. Phys.*, 2018, **20**, 3925.

76 J. Espinosa-Garcia and M. G. Chamorro, *Phys. Chem. Chem. Phys.*, 2018, **20**, 26634.

77 J. Espinosa-Garcia, J. Calle-Cancho and J. C. Corchado, *Theor. Chem. Acc.*, 2019, **138**, 116.

78 J. C. Corchado, M. G. Chamorro, C. Rangel and J. Espinosa-Garcia, *Theor. Chem. Acc.*, 2019, **138**, 26.

79 D. Troya, *J. Phys. Chem. A*, 2019, **123**, 6911.

80 D. Lu, J. Behler and J. Li, *J. Phys. Chem. A*, 2020, **124**, 5737.

81 D. Lu, J. Li and H. Guo, *CCS Chem.*, 2020, **2**, 882.

82 D. Lu and J. Li, *Theor. Chem. Acc.*, 2020, **139**, 157.

83 D. Papp, V. Tajti, T. Győri and G. Czakó, *J. Phys. Chem. Lett.*, 2020, **11**, 4762.

84 D. Papp and G. Czakó, *J. Chem. Phys.*, 2020, **153**, 064305.

85 J. Espinosa-Garcia, C. Rangel, J. C. Corchado and M. Garcia-Chamorro, *Phys. Chem. Chem. Phys.*, 2020, **22**, 22591.

86 C. Rangel, M. Garcia-Chamorro, J. C. Corchado and J. Espinosa-Garcia, *Phys. Chem. Chem. Phys.*, 2020, **22**, 14796.

87 D. A. Tasi, T. Győri and G. Czakó, *Phys. Chem. Chem. Phys.*, 2020, **22**, 3775.

88 B. Bastian, T. Michaelsen, L. Li, M. Ončák, J. Meyer, D. H. Zhang and R. Wester, *J. Phys. Chem. A*, 2020, **124**, 1929.

89 J. Meyer, V. Tajti, E. Carrascosa, T. Győri, M. Stei, T. Michaelsen, B. Bastian, G. Czakó and R. Wester, *Nat. Chem.*, 2021, **13**, 977.

90 D. Papp, J. Li, H. Guo and G. Czakó, *J. Chem. Phys.*, 2021, **155**, 114303.

91 D. Papp and G. Czakó, *J. Chem. Phys.*, 2021, **155**, 154302.

92 B. Gruber, V. Tajti and G. Czakó, *J. Chem. Phys.*, 2022, **157**, 074307.

93 B. Gruber, V. Tajti and G. Czakó, *J. Phys. Chem. A*, 2023, **127**, 7364.

94 C. Yin, V. Tajti and G. Czakó, *Phys. Chem. Chem. Phys.*, 2022, **24**, 24784.

95 C. Yin and G. Czakó, *Phys. Chem. Chem. Phys.*, 2022, **24**, 29084.

96 C. Yin and G. Czakó, *Phys. Chem. Chem. Phys.*, 2023, **25**, 3083.

97 C. Yin and G. Czakó, *Phys. Chem. Chem. Phys.*, 2023, **25**, 9944.

98 C. Yin and G. Czakó, *Phys. Chem. Chem. Phys.*, 2023, **25**, 20241.

99 C. Yin and G. Czakó, *Phys. Chem. Chem. Phys.*, 2023, **25**, 26917.

100 X. Lu, C. Shang, L. Li, R. Chen, B. Fu, X. Xu and D. H. Zhang, *Nat. Commun.*, 2022, **13**, 4427.

101 X. Lu, L. Li, X. Zhang, B. Fu, X. Xu and D. H. Zhang, *J. Phys. Chem. Lett.*, 2022, **13**, 5253.

102 D. A. Tasi and G. Czakó, *J. Chem. Phys.*, 2024, **160**, 044305.

103 T. Győri and G. Czakó, *J. Chem. Theory Comput.*, 2020, **16**, 51.

104 H.-J. Werner, P. J. Knowles, G. Knizia, F. R. Manby, M. Schütz, *et al.*, *Molpro, version 2015.1, a package of ab initio programs*, see **https://www.molpro.net**.

105 H.-J. Werner, P. J. Knowles, *et al.*, *Molpro, version 2023.2, a package of ab initio programs*, see **https://www.molpro.net**.

106 B. J. Braams and J. M. Bowman, *Int. Rev. Phys. Chem.*, 2009, **28**, 577.

107 Z. Xie and J. M. Bowman, *J. Chem. Theory Comput.*, 2010, **6**, 26.

108 H. Song, W. Xie, C. Zhang and M. Yang, *J. Phys. Chem. A*, 2022, **126**, 663.

109 R. Welsch and U. Manthe, *J. Chem. Phys.*, 2015, **142**, 064309.

110 W. L. Hase, *Encyclopedia of Computational Chemistry*, Wiley, New York, 1998, pp.399–407.

111 J. Li, B. Jiang and H. Guo, *J. Am. Chem. Soc.*, 2013, **135**, 982.

112 H. Xiang, Y. Lu, H. Song and M. Yang, *Chin. J. Chem. Phys.*, 2022, **35**, 200.

113 B. Jiang and H. Guo, *J. Chem. Phys.*, 2013, **138**, 234104.

114 H. Guo and B. Jiang, *Acc. Chem. Res.*, 2014, **47**, 3679.

115 H. Song, J. Li, M. Yang, Y. Lu and H. Guo, *Phys. Chem. Chem. Phys.*, 2014, **16**, 17770.

116 T. Michaelsen, B. Bastian, P. Strübin, J. Meyer and R. Wester, *Phys. Chem. Chem. Phys.*, 2020, **22**, 12382.

117 T. Michaelsen, B. Bastian, A. Ayasli, P. Strübin, J. Meyer and R. Wester, *J. Phys. Chem. Lett.*, 2020, **11**, 4331.

118 D. Papp and G. Czakó, *J. Phys. Chem. A*, 2022, **126**, 2551.

119 A. Y. Dymarsky and K. N. Kudin, *J. Chem. Phys.*, 2005, **122**, 124103.

120 N. I. Butkovskaya and D. W. Setser, *Int. Rev. Phys. Chem.*, 2003, **22**, 1.

**15830** | *Phys. Chem. Chem. Phys.*, 2024, **26**, 15818–15830

This journal is © the Owner Societies 2024